Chapter

Post-Fire Debris Flow Susceptibility Assessment Tracking the "Cauliflower effect": A Case Study in Montecito, USA

Johnny Douvinet

Abstract

Most of the studies focused on triggering conditions to identify the critical thresholds beyond which the occurrence of postfire debris flows becomes more than likely. However, researchers rarely focused on the relations between the morphological patterns and influences on surface water flows, while after extreme fires, the burned areas strongly reduce the infiltration capacities and generate important runoffs. So, to address these relations, we used the cellular automaton RuiCells©. This model brings out the concentration areas inside a given form, in which networks and surfaces are well-structured, and patterns are similar to efficient forms that can be found by looking at a cauliflower. This model has been applied to assess the flash floods susceptibility in sedimentary areas, with a success rate of 43%, so we decided to apply this model to the five catchments located at the apex of urbanized fans upstream of Montecito (Santa Barbara County, USA), affected by debris flows that occurred on January 9, 2018, 20 days after the Thomas Fire (one of the largest wildfires in California history). Some of values have never been observed elsewhere. So, we might apply this approach to assess the postfire debris flows susceptibilities given the increasing number of fires and mega fires.

Keywords: debris-flows, postfire conditions, spatial behavior, Montecito

1. Introduction

Given projected increases in wildfire size and severity [1], precipitation intensity and variability [2, 3], or in development in the wildland-urban interface [4], there is a growing need to increase resilience to disasters [5] and to reduce as far as possible impacts of hazards on lives, properties, bridges, roads, and infrastructures [6]. Postfire debris flows are phenomena able to rapidly transport large volumes of sediment and large boulders, sometimes over long distances, making surface flows destructive and dangerous [7–9]. The debris flow dynamics are determined by solid and fluid forces, while in floods and hyper-concentrated floods, the dominant

process is more determined by fluid forces alone [10]. The transition between processes represents a spatial and temporal continuum: one single event is often related to different pulses that have different characteristics [11]. Furthermore, the flow properties vary along the course of the channel with the lower channel reaches often exhibiting flood characteristics due to increased sediment deposition rates as well as dilution from increased water content relative to the sediment entrainment rate [12, 13].

Currently, evidence has emerged on postfire rainfall thresholds and the relations between convergence zones and preexisting drainage lines [14], which results in rapid channel development where bedrock eventually set the lower limit of scour depth. Immediately after a fire, the role of overland flow during rains becomes magnified due to losses of vegetation [15, 16], changes in soil properties, and sediment supply [17]. Thresholds are significantly lower than most identified for unburned settings, due to the difference between rapid runoff-dominated processes acting in burned areas, and longer-term, infiltration-dominated processes on unburned hillslopes [9]. However, the hydro-geomorphic response of burned upland regions can be variable. It depends on various factors including the fire severity, timing, and properties of postfire rainfall events, as the inherent geomorphic and hydrological characteristics of fire-affected catchments [1, 3]. Debris flows or sediment-laden floods are produced from the small burned catchments, in response to short rains and convective thunderstorms in the intermountain west U.S. [18–20], and to longer duration winter frontal storms in southern California [21, 22]. Therefore, unlike landslide-triggered debris flows, these events have no identifiable source, and they can occur with little or without moisture.

However, researches rarely focused only on the links between the morphological patterns and influences on surface water flows, while after extreme fires, the burned areas strongly reduce the infiltration capacities and generate high Hortonian runoffs. Indeed, the debris flow susceptibility still remains assessed by considering the slope, curvature, elevation, or terrain complexity as secondary factors [23, 24]; meanwhile, the impacts of network and surfaces, organized within a given form, are neglected, whereas the morphological effects play a strong influence during postfire conditions.

To overcome such a problem, this study proposes to apply a methodology that we have already tested in the situation of high Hortonian runoffs [25–27]. The cellular automaton (so-called RuiCells©) is used to track efficient points upstream of which networks and areas are well-structured, and patterns are similar to efficient forms that can be found by looking at a cauliflower. This model has been applied in France to assess the flash flood susceptibility in sedimentary context, with a success rate of 43%, so we decided to apply this model in other areas or for more extreme events such as postfire debris flows. If results are positive, this model could then bring a new way to assess the postfire debris flows susceptibilities in more catchments.

After presenting the five studied catchments and the 2018 debris flow features (Section 2), the method and data used are described (and especially the "cauliflower effect") in Section 3. Results are described by following two observation levels: the morphological signatures obtained at the global scale and the "cauliflower effect" detected at fine scales (Section 4). The discussion continues by focusing on the relations between the importance of burned areas and usefulness of debris basins, in relation to the "cauliflower effect" and morphological influences (Section 6).

2. Hydrological data and studied catchments

2.1 Study area

Located 8 km east of Santa Barbara, Santa Barbara County, California (USA) (**Figure 1**), Montecito is an unincorporated community and a census-designated place. The population was estimated in 2018 to be 9145 residents, and Montecito is regularly ranked by the Forbes magazine as one of the wealthiest in the United States (2016, 2017). According to the magazine, it is 21 of the 100 most influential public figures in the United States are known to own property (2017). The climate is characterized by warmer winters and cooler summers, compared with places further inland, because of the ocean's proximity [5, 28]. Located at the foot of the Santa Ynez Mountains, which are mostly of sedimentary origin, the peak relief has an altitude of 981 m. Several creeks span approximately 3 km between the mountain front and the Pacific Ocean, intersecting State Route 192 and Highway 101. Since distances between mountains and bay are shorter, steep terrain presents hillslope gradients: ~37% of the terrain exceeds 35 degrees, and creek-bed gradients are ~12% [5]. Under these conditions, surface runoff and waters rapidly flowed south into a series of creeks with gradients of ~5%, and drain south through the residential city of Montecito, with construction in a series of alluvial fans [29, 30]. The urbanized piedmont plain contains steeply sloping alluvial-fan landforms generally north of State Road 192 and Highway 101 and gently sloping alluvial-fan landforms near the coast. And to protect the high density of roads and structures on the alluvial fans, four sediment-retention basins have been built along the main paths: Cold Spring (1964), San Ysidro (1964), and Romero (1971), as recorded by Santa Barbara County.

2.2 Awareness of the risk of debris-flows

Before the 2018 event, Montecito had a high level of situational awareness prior to the storm [5]. Historical and damaging debris flows (1926, 1934, 1964, 1969, 1971, 1990, and 2002) have been already registered [31, 32], and debris flows became a

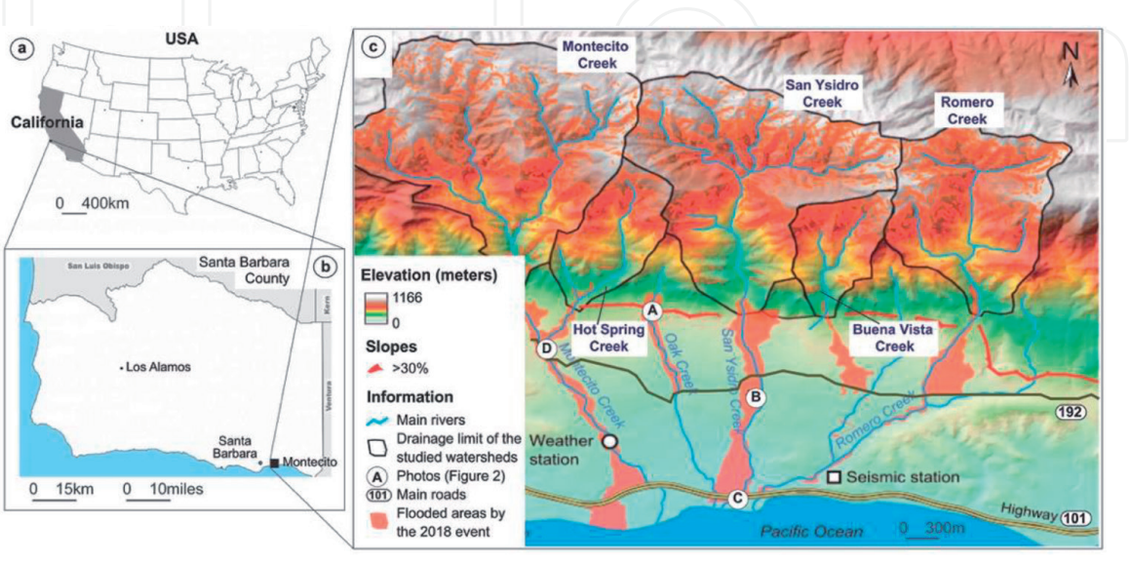

Figure 1.
Location of the five studied catchments (with damage extracted from 31).

Catchment Name	Catchment area (km^2) – *A*	Basin slope (50th, 90th percentiles)	Area burned at moderate to high severity (%)	Predicted likelihood for design storm. (I_{15} = 24 mm/hr)
Montecito Creek	14.07	28/39	79	65%
Hot Spring Creek	3.34	28/40	49	70%
San Ysidro Creek	11.63	28/40	85	69%
Buena Vista Creek	2.66	29/41	82	63%
Romero Creek	7.11	30/42	78	62%

Table 1.
Indicators confirming the high probability for a postfire debris flow in Montecito just before the 9 January 2018.

topic of research since the 1934 debris flow in Montrose that killed over 40 people [29, 30]. Some researchers documented the sediment-laden water flow following the 1990 Painted Cave fire, and they have proven that the first few months following wildfire are of most concern [29, 30]. Awareness of the debris flow risk was emphasized by coordinated efforts between county, state, and federal agencies that included: (1) a determination of the soil burn severity as a good indicator of flooding and debris-flow potential [33]; (2) the debris-flow hazard assessment that shows the high likelihood and potential volume of debris flows from the burned areas, in response to design storms [34]; a warning system that predicted significant to the extreme potential for debris flow in the 4 days leading up to the storm [35, 36]; and (4) a proactive emergency community that coordinated evacuation orders to reduced casualties [5]. However, despite these efforts, it remains hard to anticipate such events: (1) assuming the annual probability of a wildfire in this area (following recovery from a previous fire rated at 0.10), and that the probability of a short duration high intensity storm is 0.02, the conditional probability is 0.002 [29, 30]; (2) prior to the 9 January 2018 rain event, the U.S. Geological Survey (2018) had predicted a 62–70% probability of debris flows from the five catchments located in upstream Montecito (**Table 1**) for a design rainstorm of I15 = 24 mm/hr. [34], but forecasting such intensity remains difficult in real time.

2.3 Characteristics of the January 2018 event and hydrological data

The Thomas fire above Montecito burned from the ridge crest of the Santa Ynez Mountains on December 2017 (from the 14th until the 27th), to approximately the apex of the urbanized alluvial fans [5, 6, 29, 30]. Under these conditions, the occurrence of debris flows was feared, and rainfalls were watched [37]. Early on the morning of 9 January 2018, a heavy rain characterized by high intensity (13 mm in 5 min, e.g. 157 mm/h) at 3.45 a.m. (recorded by the Montecito rain gauge) caused flows consisting of mud, boulders, and tree branches up to 15 feet (up to 5 m) in height, and moving at estimated speeds of up to 20 miles per hour (around 30 km/h) into the downstream creeks, valleys, and lower areas of Montecito [38]. A few minutes later, at 3:47 a.m., the Montecito Fire Department received the first calls of a major explosion on San Ysidro Creek–East Mountain Drive [5]. Flows on Cold Spring Creek began at 3:49 a.m. (this was confirmed by the security camera footage). Inundations began on the northern plains of Montecito around 3:50 a.m., and estimated lag times are estimated ranging from 4:06 to 4:10 a.m. [39], with the seismic signature of debris flows. The rainfall threshold for the occurrence of debris flows decreased obviously due to the Thomas Fire and the percent of burned areas, ranging from 49% within Hit

Catchment Name and number	Catchment area (km^2) – *A*	Accumulation Area (km^2) – AA	Inundated Area (km^2) – IA	Estimated Sediment Volume (m^3) - OSV
Montecito Creek	14.07	0.78	0.997	231,000
Hot Spring Creek	3.34	0.08	0.102	10,000
San Ysidro Creek	11.63	0.69	0.905	297,000
Buena Vista Creek	2.66	0.11	0.290	41,000
Romero Creek	7.11	0.17	0.312	100,000

Table 2.
Data collected during the 2018 Montecito event [5, 6, 34, 37].

Spring Creek to 85% in San Ysidro Creek (**Table 2**). No floods occurred on 9 January 2017 (for cumulative precipitation of 16.5 mm), whereas several debris flows occurred on 9 January 2018, with cumulative precipitation of less than 13.7 mm in 5 min [28]. And the sediment basins do not limit the violence of flows.

The 30-foot wall of boulders, mud, and debris flows ran down hillsides at 15 miles per hour, injuring dozens and causing 21 prehospital deaths and 2 missing persons (two children of 17- and 2-year old's). 163 people were hospitalized for injuries [40] and a retroactive review conducted of 24 victims from the debris flows presenting to Cottage Health showed that most part of symptoms referred to soft tissue injuries (100%), hypothermia (67%), craniofacial injuries (67%), corneal abrasions (53%), and orthopedic injuries (47%), as well as the loss of an immediate family member (73%) because of the incident [40]. Around half of the victims who perished were migrants from working-class families [28]. Hopefully, crews rescued at least 50 people by air, dozens more from the ground, and 300 people stocked in their homes along the Romero Canyon neighborhood after impassable roads halted rescue operations, the disaster caused $177 million of insured property damage, $7 million in emergency responses, and $43 million in cleaning costs [41, 42], with a final cost approaching more than $250 million in 2019 [5].

Although creeks are incised by more than 5 m into the surrounding terrain (**Figure 2**), the debris flows overflowed the valleys, often at bridge crossings, and carried boulders into the neighboring residential areas [5]. The debris flow deposits cover around 7 km^2 and the cumulative amount of sediment are ranging from 297,000 m^3 [33], 680,000 m^3 (including boulders up to 6 m. in diameter) to up to 880,000 m^3 [34]. Damage was concentrated within the 500-meter-wide flow path in numerous areas, and was mostly pronounced along the Montecito and San Ysidro Creeks, as 80% of the 408 damaged and destroyed homes were located in them. Additionally, flow bifurcated approximately 0.7 km downstream of the mountain front and traveled in a southwest direction from San Ysidro Creek, along El Bosque Road [37]. Finally, debris flows resulted in damage to at least 163 structures and complete destruction of an additional 92 structures.

3. Methodological assessment

To complete researches that have been already carried out on the 2018 Montecito event [5, 35–39], the deterministic cellular automaton so-called RuiCells© was used.

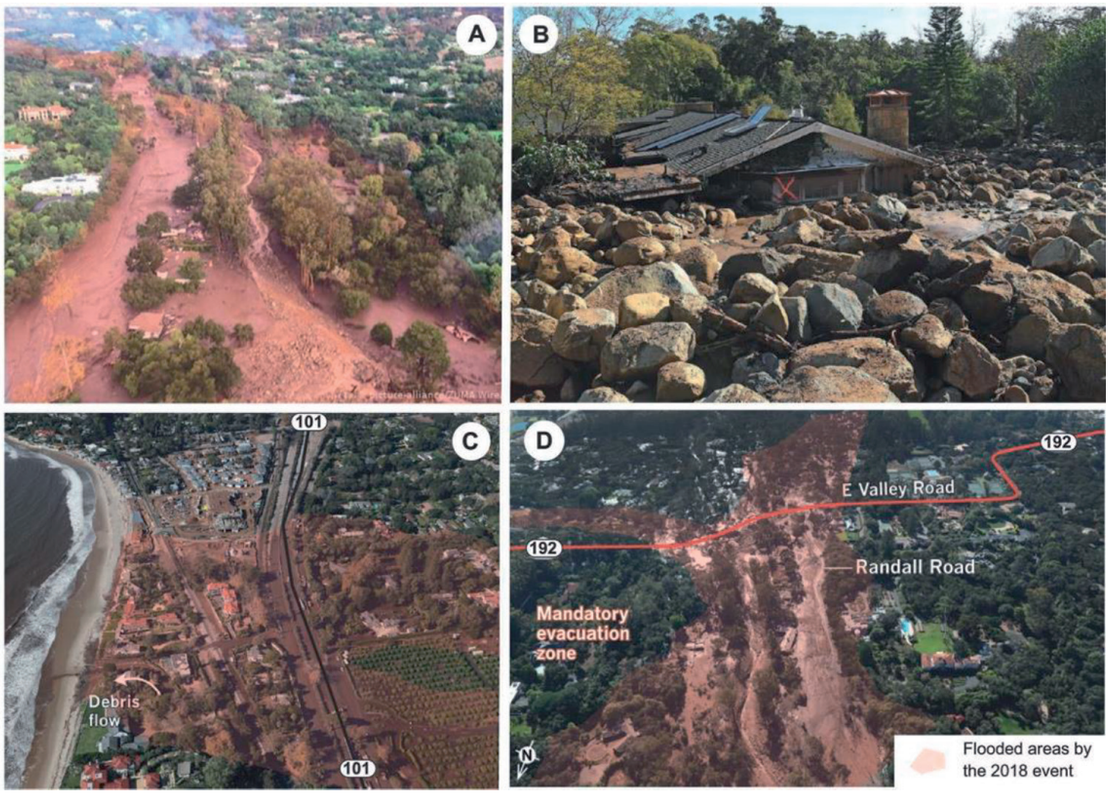

Figure 2.
Damage and spatial extent of debris flows in 2018 in Montecito.

First, to further assess the dynamical influences of morphological conditions on the sudden hydrological responses of the catchments located upstream of alluvial fans. Any morphometric parameters have been reported to be related to debris flow potential [25, 26], but their usefulness is limited and often criticized [27]. Second, to track the points in upstream of which areas and networks are well organized (the so-called "cauliflower effect"). Simulations give a picture of the "*width function area*" [25, 27], but concentration area or internal efficiency can be detected, and this effect could explain violent hydrological responses, in time and space.

3.1 The "cauliflower effect" and its links with hydrological features

The series of processes from the cause generating a cauliflower form is complex. One might assume that the underlying rules for the cauliflower growth are simple, even if the form is of great complexity [43]. But the crucial phenomenon that ultimately leads to much of the structure is that at the tip of a stem is possible for new stems, to form and branch off. In the simple cases, these new stems are in essence just smaller copies of the original stem. With this setup, the branching succession can be represented by steps in the evolution of a neighbor-independent substitution system. The cauliflower finally presents an unusual phyllotaxis, with a multitude of spirals nested over a wide range of scales. This self-similar organization culminates in the Romanesco cultivar, where the spirals appear in relief due to their conical shape at all scales, a geometrical feature conferring the whole curd a marked fractal-like aspect [43].

Similarities can be found by comparing forms of cauliflower and hierarchical river organization: without geological or lithological constraints, a stream river branching progress through scales [44], and if the distance before the stream appears is

determined by the rates of production or the erosive capacity of waters, a minimum area is needed for elementary catchments [45]. The layout of the network becomes fundamental considering the path and transit time, from the source to the outlet. The *width function* created by [46] has permitted consideration of the number of hydrological links located at equal distances from the outlet [46], thus taking into account the network and the surfaces within a given watershed form. This function remains today one of the most relevant tools, to link the shape of a basin and its hydrographic network, to the hydrological response resulting from this organization [25, 27], even if numerous works have improved the calculation and the method of extraction of this function, by associating the slopes. A structurally well-organized network finally presents, without external constraints, a form nearest to those of a cauliflower: it represents a homothetic phenomenon, with a minimal dispersion of energy, which reminds the "self-organized critical systems" [47]. But the global catchment form can be hidden on the global scale. Then, we create a specific model to measure this effect.

3.2 Simulation of the "cauliflower effect" with the RuiCells© model

To address the "cauliflower effect," we used a specific cellular automaton so-called RuiCells, that has been already described before [26, 27]. For this specific simulation, we simulate the sum of surfaces flowing within networks. Cells at the beginning of the simulations are initialized with their surface (defined by the TIN and depending on the DEM resolution, here 50 m as previous studies have been calibrated on this). RuiCells© handles the advection operator in moving surfaces between each cell, so a formal property defined in classical CA is maintained [48], as transition rules operate on cells based on local neighborhood. Surface flow is routed via each cell until the downstream boundary is reached [48]. At the end of the simulation, a graph presents sum of surfaces registered at each interaction to present the morphological signature of the basins, defined as a function of distance *n* from the outlet (**Figure 3**). Steps are length steps since the surface flow diffusion depends on the spatial lattice size. These surface flow graphs give the 2D theoretical spatial behavior of a catchment. This improves older methods, that only informed on the number of links in the network at a flow distance x to the outlet [46], as areas flowing in RuiCells© follow hydrological rules (differences between surface, linear, or node transition are accounted), and are based on a triangular lattice.

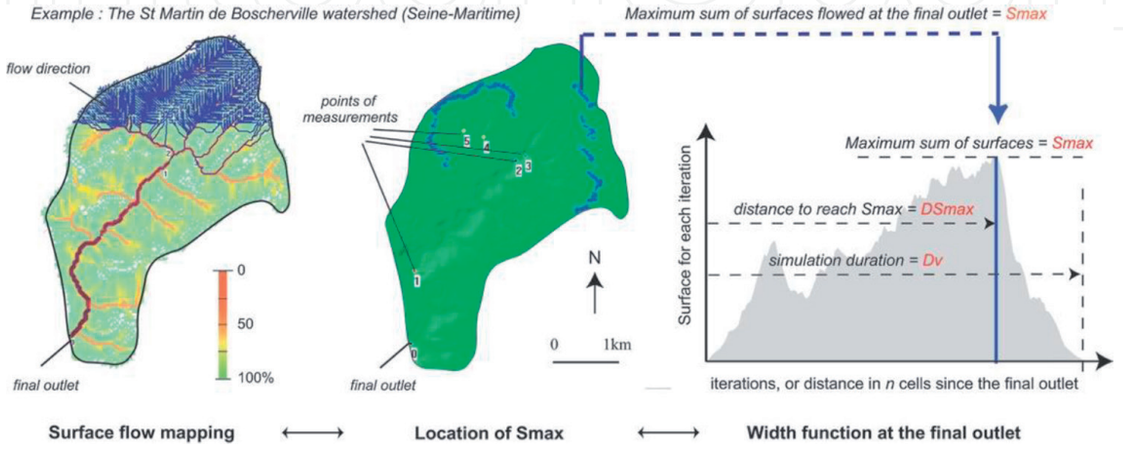

Figure 3.
Sum of surfaces per iteration, simulated by RuiCells©.

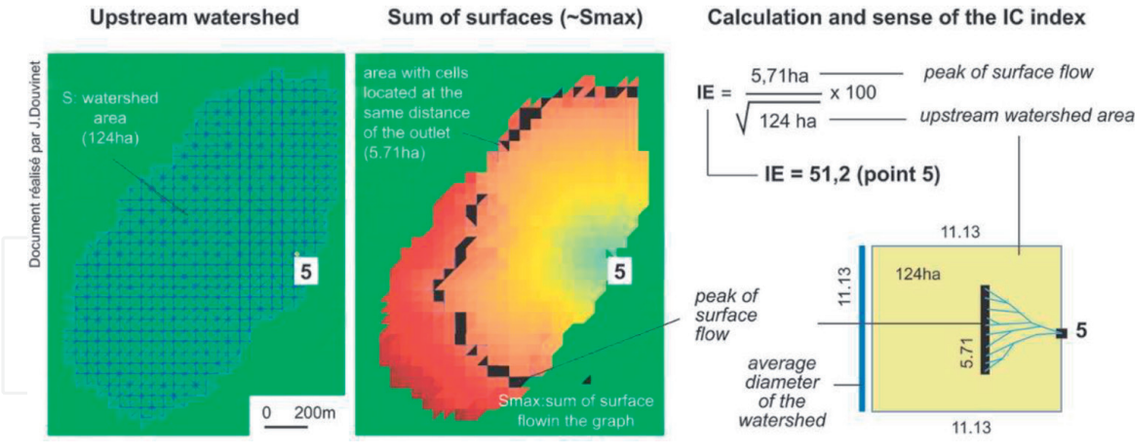

Figure 4.
The concentration index (CI) estimated by the RuiCells© model.

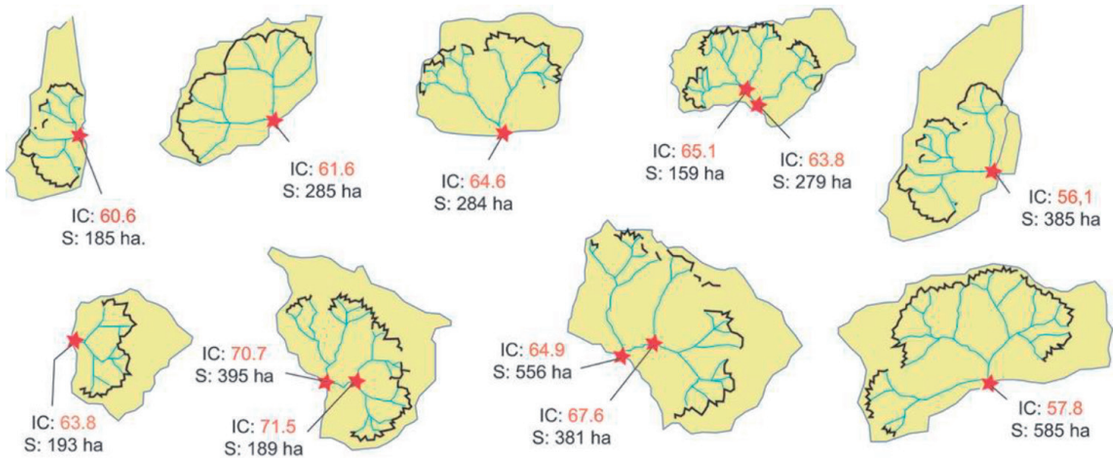

Figure 5.
Line of SMax in catchments where runoff concentrate in a short distance (according to Douvinet, 2008): the so-called "cauliflower effect."

In addition, to track the "cauliflower effect," the highest sum of surfaces (*Smax*) is divided by the square root of the catchment area (A') located upstream (**Figure 3**), to define a Concentration Index (CI). *Smax* equals to the highest line of cells located at a distance n from the point of measurement. As *Smax* is related to a length (since the square root equals to the average diameter of the upstream area), CI is dimensionless (**Figure 4**). Values are automatically calculated during the simulation process and are mapped. Strong values (colored in red) identify the neuralgic points inside the basin where the network is very effective with respect to the shape in which it is inserted. Values have the same significance regardless of the basin area if the TIN resolution never changes. In this approach, we always use a DEM of 50-m long. If CI equals to 50, it indicates a medium flow concentration: the peak of surfaces (*Smax*) corresponds to half of the average diameter. But if CI values exceed 55, networks and surfaces appear highly well-structured [25]. If strong values are observed, the efficient line of cells *Smax* is mapped, and a perfect form (so-called the "cauliflower effect") appears. Examples (**Figure 5**) illustrate this in previously studied catchments: red stars located the efficient points, blue lines some of the branches of the networks, and black lines the surfaces. Points

and linear with IC > 55 concentrate high surface flows in a short distance, with a minimum energy expenditure [27, 47].

3.3 Prospects and limitations

Simulating the influence of morphological conditions on hydrological responses is limited for a few reasons: (1) this theoretical approach cannot be compared with real simulation results obtained with more pervasive models; (2) the efficient points can be located within catchments where no violent floods occurred (probably due to the lack of intense rains); (3) sediment production is not combined with water production, while these processes could complexify the real hydrological response.

Estimating the "cauliflower effect" in the five catchments located at the apex of the Montecito may, however, allow: (1) to check if the erosive areas are related to sudden debris flows and important damage; (2) to compare information supported by the "cauliflower" effect to other results. If the model identifies real sensitive areas, it could extend the model's usefulness and the scope of the model. If the model identifies sensitive areas that have not experienced severe flooding, the rainfall can have not been sufficient to cause them to respond, and the lack of correlation could raise concerns about a future event. If the model does not identify sensitivity in areas that have been affected, the relevance of this model may be excluded, and the morphometric factors should be excluded as efficient, to look for the origin of the susceptibility in the other variables (soil, burned areas, rain, exposure...). This validation process finally allows us to know if RuiCells© can be useful for the decision-makers in the era of extremes, to whom we could say: then, "if you observe a cauliflower effect in a burned catchment, be very careful in case of rains!"

4. Results

4.1 Morphological signatures and role of internal organization

The spatial behaviors simulated at the outlet of the five basins are first studied. Several points of measurements have been added within the biggest basins, to further understand the genesis of the simulated sum of surfaces. In the Montecito Creek basin (**Figure 6**), the surfaces located upstream the points 2 and 3 support together the *SMax* measured at the final outlet (**Table 3**), around the 100th iteration. This catchment presents a high IC value at the final outlet (55.74), due to the hierarchical organization of networks. Such efficiency is more effective in the San Ysidro Creek (**Table 3**): many surfaces flow since the upstream part of the point 7, and numerous surfaces are drained thanks to the well-structured networks. In Hot Spring or Buena Vista Creek, the cascading surface flow system is slightly less inefficient as the contributions of sub-basins are shifted in space. As a consequence, values for *Smax* are lower. In Romero Creek, upstream areas of the point 10 present an efficient organization, but their contribution is not combined with other sub-basins at the final outlet, explaining the small value for *SMax* at the final outlet (**Figure 6**). A similar discrepancy induces in Hot Spring Creek a long out-flow. Obviously, the *SMax* value in upstream point 1 in the Montecito Creek is close to those obtained in upstream points 10 and 3 (**Figure 6**), but as they are not spatially combined, no major peak of surfaces can appear.

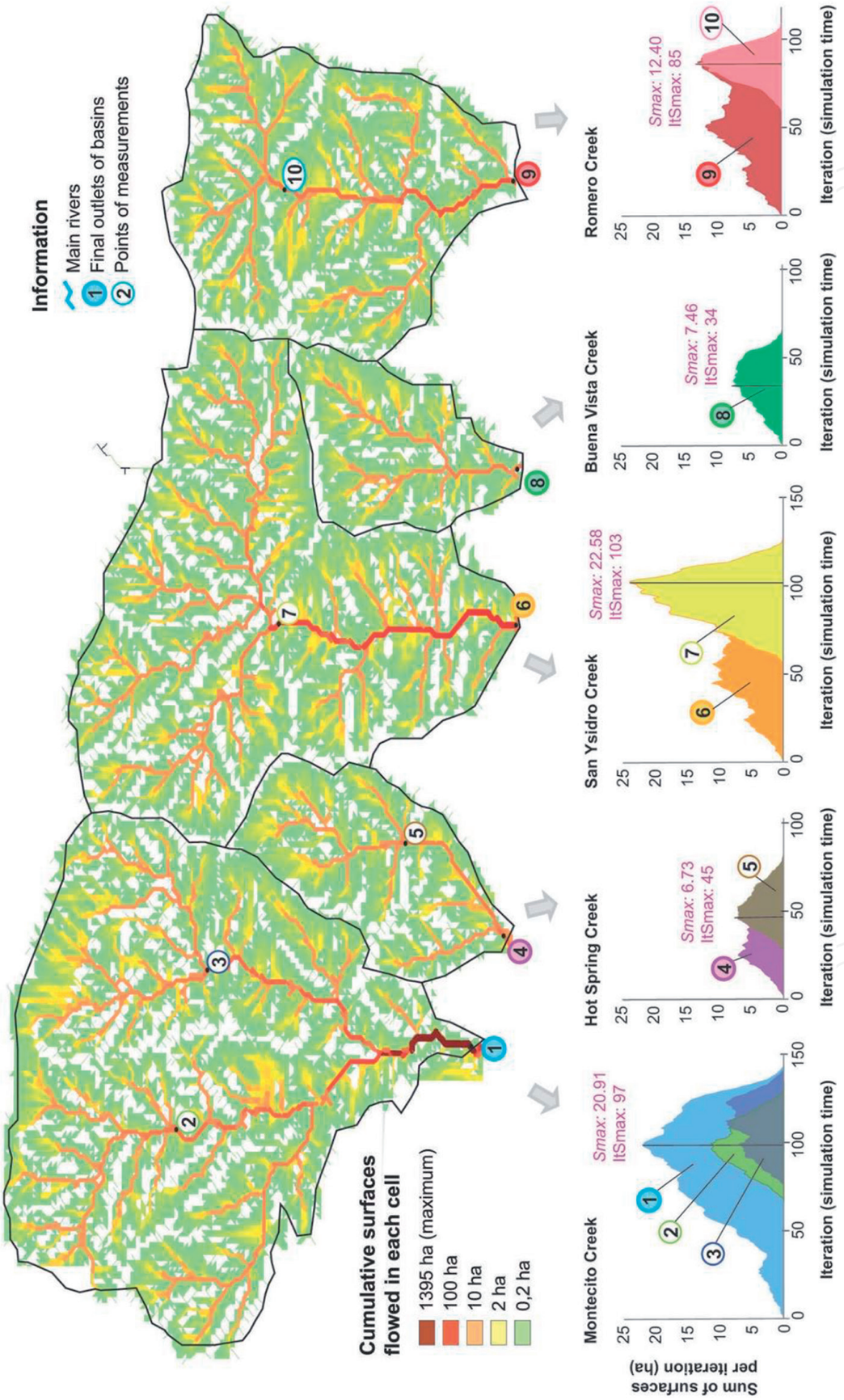

Figure 6.
Simulated surface flow response in the five studied catchments.

Catchment Name and number	Catchment area (km^2) (*A*)	Time for the simulation (It)	Maximum sum of surfaces (*Smax*)	Iteration of Smax (It*Smax*)	CI value (outlet)
Montecito Creek	14.07	147	20.91 ha	97	55.74
Hot Spring Creek	3.34	89	6.73 ha	45	36.80
San Ysidro Creek	11.63	133	22.58 ha	103	66.21
Buena Vista Creek	2.66	82	7.46 ha	34	45.74
Romero Creek	7.11	112	12.40 ha	85	46.50

Table 3.
Outputs collected at the final outlet of the five studied catchments.

This first analysis then confirms that the global catchment scale is not relevant to address the effects of morphological conditions on hydrological responses, especially for the five studied catchments: for example, the upstream part of point 7 explains 100% of *Smax* estimated at the final outlet (point 6), while its surfaces only represent 64% of the global basin size (11.63 km^2). So, we need to track concentration within networks at a finer scale, hence the interest in going down to the cellular scale.

4.2 The "cauliflower effects"

Maps indicating values of Smax at the cellular scale confirm that strong high values (IC >55) exist within the catchments (**Figure 7**). A very important value (IC = 81.1) is simulated within the San Ysidro upstream part (Smax: 22.58 ha; A: 7.74 km**2**), and this record has never been observed elsewhere and in previous studies. Indeed, even if RuiCells © has been applied on more than 450 catchments in France [49], the older maximum value was estimated in Saint-Martin-de-Boscherville (in France), with IC equal 71.6. In this study, for San Ysidro Creek, the internal efficiency was already suggested (**Figure 6**), but the "cauliflower effect" is remarkable: the contribution of three well-structured sub-basins suddenly increases the IC values, as they contribute together and surfaces arrive at the same moment in upstream of the point 7. IC values remain higher (>55) until the final outlet is reached (**Figure 8**), which indicates that surface flow is efficient during a distance of around 1.125 km. The number of branches and their similar distance to the outlet aggravate hydrological responses and support current solid debris content, especially during the postfire conditions.

In Romero Creek, another IC high value is clearly detected (IC = 76.9; Smax: 12.40; A: 2.65 km**2**), while IC was weak at the outlet (IC = 46.50). Here, the rest of the catchment does not play a role in the surface response. In Montecito Creek, several IC values appear, and they exceed the threshold value of 55 (57.8 at the point 2 and 58.4 at the point 3). One homothetic behavior is observed: efficient concentration areas emerge in different confluences in the river system, and this explains why a distance of 450 m (red-colored) upstream of point 0 still has a morphological efficiency. And finally, morphology in the Buena Vista and the Hot Spring Creeks seem to be less effective. In fact, the two basins present an internal concentration, but values are weaker (53.1 and 52.1) in comparison with others, so their morphological efficiencies are hidden by other extreme values.

As a consequence, the "cauliflower effect" is detected, and it gives new patterns to the relations between networks and areas (**Figure 8**), completing the previously

Figure 7.
Maps of IC index in the five studied hydrological catchments.

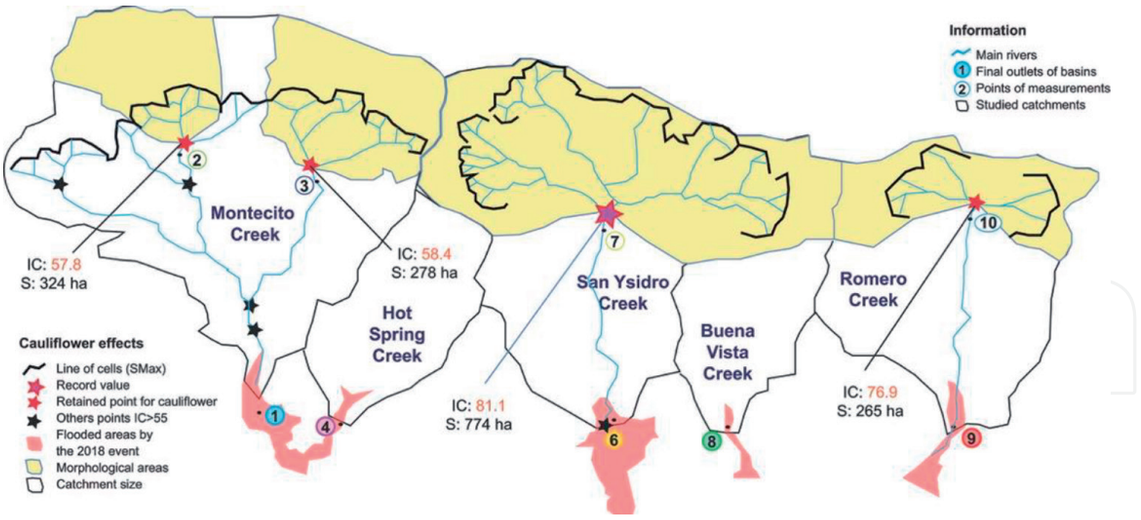

Figure 8.
The "cauliflower effect" in upstream morphological areas.

known forms (**Figure 5**). More networks and surfaces are numerous and equidistant from the outlet point, more this "cauliflower effect" takes sense as shown by the form around the new record point. The morphological areas often do not correspond to the global catchment scale, that is why the global scale is not relevant to address the morphological influence on surface flow dynamics. And it also explains with morphometric parameters (calculated for a given form or size) are really insufficient to detect their influence in case of violent and sudden events like debris flows.

5. Discussions

5.1 Insights related to previous flash floods collected data

Additionally, we compared simulation results with various data collected in other studies. Human damage was really dramatic at the final outlet of Montecito and San Ysidro Creeks: along the 1st 1 km of these two catchments from the apex, debris-flow stages were several meters above the channel banks, and at some locations exceeded 10 m above the initial thalweg [5]. By the way, our simulations demonstrate the good performance of RuiCells© model, which exhibits high morphological efficiency and the role played by morphological signature. Due to the intense efficiencies and the burned surface, conducive to hortonian runoff, debris flows arrived suddenly and violently at the interface between the final outlets and first homes located at the apex. The high burned areas (respectively, 79 and 85%) added to morphological efficiencies have also aggravated the quick responses (**Table 1**). Complementary simulations with RuiCells© [49] also proved that the rainfall intensity played a tiny role in the increase in runoff flows and volumes (1.4 to 1.86, if comparing 2017 and 2018 rainfall with no fire impacts). By injecting the 2018 rainfall and the magnitude of the burned areas (from 83 to 79% in San Ysidro, Montecito, and Romero), we estimate that fire and morphology combined with rainfall increase peak flows by orders of magnitude ranging from 9.7 to 10.3. On the other hand, other geomorphological indicators also confirm that the "cauliflowers effects" are not fictive. Large boulders (with a-axis > 1 m) were transported nearly the entire length of San Ysidro, Montecito, and

Romero creeks. But numerous locations of boulder deposits coincide with human infrastructure, roads, clogged culverts, bridge underpasses, or variations in the channel slopes. But surely all these damages are related to high water velocities and capacities, so indirectly to high concentration. And finally, topography really seems to be the key factor to assess postfire debris flows [29, 30, 34, 40].

5.2 Challenges face in the current era of extremes

The outcome of the 2018 postfire debris flow event that took place in Montecito was devastating but could have been worse if no coordination had taken place between the local, State, and Federal Agencies and if no early warning had been issued by the NWS or Santa Barbara OEM. However, our new simulation results can be used to produce a simple heuristic approach and be relevant to the existing "Duck, Cover, and Hold" for earthquakes. We might use "wildfire – intense rain – move uphill," or "Ready" (be prepared in advance to evacuate if necessary), "Set" (monitor fire burned areas and postfire precipitation in preparation to evacuate), and "Go" (evacuate when directed or if you are uncomfortable). These terms are in the Santa Barbara County hazard education program [50], and drills are currently being tested in elementary schools in Montecito as part of hazard education [29, 30]. More suitable, during the 2018 event, many people did not comply with the evacuation order required by local stakeholders, and errors detected in the past were not taken into account by many actors. Understanding why people do not comply with evacuation orders concerning debris flows is key to knowing how to better communicate the risks in ways that may lead to better disaster preparedness and response. And even a slight delay in starting your evacuation will result in significantly longer travel times as traffic congestion worsens [50]. Therefore, the challenge still remains in identifying the exact timing and location where intense convective cells might develop (isolated or within a larger system). The 2018 event featured a north–south oriented atmospheric river with two moisture bands interacting with a closed low-pressure system. The main AR had moved southeast by the time of the debris flows. While the NCFR drove the high rain rates that produced the debris flow, the AR helped transport moisture into the area. Across the Santa Ynez and Topatopa Mountains, approximately 2–5+ inches of rain fell over a 2-day period. This value indicates a moderate storm for the region in terms of precipitation totals. However, the NCFR produced periods of intense rain. The 15-minute rains observed correspond to a 25–50 years event according to NOAA, while the FS model reported a 15 min total of 0.86 inches, a 100-year event [51].

6. Conclusions

The occurrence of the debris flows in Montecito in 2018 were not a surprise, but the magnitude and impacts of the flows were. Before the rains arrived, first responders were prepositioned, evacuations were implemented, a proclamation of emergency was executed at local scales and the operations center was staffed. However, despite technical or engineering advances, such sudden events occurred after extreme fires, and the susceptibility as thresholds indicating their probable occurrence could not be adapted to this remarkable situation. In addition, the Montecito event highlighted the need to develop more refined models that can be used in the field to accurately identify the risk and map debris flow inundation zones. Being able to map the hazard and

related risk help convey this critical information to decision makers to implement mitigations and appropriate emergency measures, such as issuing an evacuation alert. Decision makers need to have confidence and be able to point to the science that what they are doing is proper and prudent. On the other hand, the studied catchments were investigated as a new example to detect a possible "cauliflower effect," and these new results confirm the influence of morphological conditions playing a key role in real postfire debris flow events. In the era of extremes, intense rainfall intensities are expected (at daily and not annual scales) but coupled with severe dry periods and severe fires, runoff concentration and violent hydrological responses could occur and surprise many people located at the outlet of small catchment. Thus, even if RuiCells© model should be more calibrated, we propose to assess such risk considering that catchments are totally burned, and the detection of "cauliflower effects" is finally not so theoretical. And to follow this study, we plan to measure this effect on the other postfire debris flows that occurred in California, with a set of 334 events of events.

Acknowledgements

The author addresses his sincere thanks to Anna Serra-Llobet, John Radke, and Matthias Kondolf (working at Berkeley), with whom he worked, and for the meeting organized the 6 February 2020 in Berkeley, with crisis managers and scientists, just before the international pandemic crisis. He also thanks Daniel Delahaye (University of Caen, France) and Patrice Langlois who create the RuiCells© model. He also thanks the institutions who financially supported this research: the France Berkeley Fund, for funds obtained in 2019; Avignon University, for support in 2022; and the Institut Universitaire de France (IUF), for grants over the period 2021–2026.

Author details

Johnny Douvinet
Avignon University, Avignon, France

*Address all correspondence to: johnny.douvinet@univ-avignon.fr

References

[1] Westerling A, Hidalgo H, Cayan D, Swenam T. Warming and earlier spring increase forest wildfire activity. Science. 2006;**313**:940-943. DOI: 10.1126/science.1128834

[2] Donat M, Lowry A, Alexander L, Ogorman P, Maher N. More extreme precipitation in the world's dry and wet regions. Nature Climate Change. 2016;**6**:508-513

[3] Swain D, Langenbrunner B, Neelin JD, Hall A. Increasing precipitation volatility in twenty-first-century California. Nature Climate Change. 2018;**8**:427-433

[4] Cannon S, DeGraff J. In: Sassa K, Canuti P, editors. The increasing wildfire and post-fire debris-flow threat in western USA, and implications for climate change, Landslides—Disaster Risk Reduction. Berlin, Heidelberg: Springer; 2008. pp. 177-190. DOI: 10.1007/978-3-540-69970-5_9

[5] Kean J, Staley D, Lancaster J, Rengers F, Swanson B, Coe J, et al. Inundation, flow dynamics, and damage in the 9 January 2018 Montecito Debris-flow event. California, USA: Opportunities and challenges for post-wildfire assessment. Geosphere. 2019;**15**:1140-1163. DOI: 10.1130/GES02048.1

[6] Cui Y, Cheng D, Chan D. Investigation of post-fire debris flows in Montecito. Geo-information. 2019;**8**:5. DOI: 10.3390/ijgi8010005

[7] Coe J, Kean J, Godt J, Baum R, Jones E, Gochis D, et al. New insights into debris-flow hazards from an extraordinary event in the Colorado Front Range. GSA Today. 2014;**24**(10):4-10. DOI: 10.1130/GSATG214A.1

[8] Takahashi T. Debris Flow: Mechanics, Prediction and Countermeasures. London, UK, Taylor and Francis; 2007. DOI: 10.1201/9780203946282

[9] Cannon S, Gartner J, Rupert M, Michael J, Staley D, Worstell B. Emergency Assessment of Postfire Debris-Flow Hazards for the 2009 Station Fire. San Gabriel Mountains, Southern California: U.S. Geological Survey Open-File Report; 2009. p. 27

[10] Costa J. Rheologic, geomorphic, and sedimentologic differentiation of water floods, hyper-concentrated flows and debris flows. In: Baker VR, Kochel RC, Patton PC, editors. Flood Geomorphology. Chichester: John Wiley & Sons; 1988. pp. 113-122

[11] Pierson T. Distinguishing between debris flows and flows from field evidence in small watersheds. U.S. Geological Survey Fact Sheet, 2004-3142. 2005

[12] Hungr O, McDougall S. Two numerical models for landslide dynamic analysis. Computers & Geosciences. 2009;**35**:978-992. DOI: 10.1016/j.cageo.2007.12.003

[13] Meyer G, Wells S. Fire-related sedimentation events on alluvial fans, Yellowstone National Park USA. Journal of Sedimentary Research. 1997;**67**(5):776-791

[14] Fuchs S, Kaitna R, Scheidl C, Hubl J. The application of the risk concept to debris flow hazards. 2008:120-129. Available from: http://wwwdsireusaorg/ (in English)

[15] Wondzell S, King J. Postfire erosional processes in the Pacific Northwest and

Rocky Mountain regions. Forest Ecology and Management. 2003;**178**:75-87

[16] Parise M, Cannon S. Wildfire impacts on the processes that generate debris flows in burned watersheds. Natural Hazards. 2012;**61**(1):217-227

[17] Moody J, Martin D, Cannon S. Post-wildfire erosion response in two geologic terrains in the western USA. Geomorphology. 2008;**95**:103-118

[18] Nyman P, Sheridan G, Smith H, Lane P. Evidence of debris flow occurrence after wildfire in upland catchments of south-east Australia. Geomorphology. 2011;**125**(3):383-401

[19] Parrett C. Fire-related debris flows in the Beaver Creek drainage, Lewis and Clark County, Montana. In: Subitzky S, editor. USGS Water Supply Paper 2330, Denver CO. 1987. pp. 57-67

[20] Cannon S, Gartner S. Runoff and erosion generated debris flows from recently burned basins. Geological Society of America Abstracts with Programs. 2005;**37**(7):35

[21] Wells W. The effects of fire on the generation of debris flows in southern California. In: Costa JE, Wieczorek GG, editors. Debris Flow/Avalanches: Process, Recognition, and Mitigation. Reviews in Engineering Geology. Vol. VII. Boulder, CO: Geological Society of America; 1987. pp. 105-114

[22] Booker F. Landscape and management response to wildfires in California: [MSc thesis], University of California, Berkeley. 1988

[23] Archetti R, Lamberti A. Assessment of risk due to debris flow events. Natural Hazards Review, American Society of Civil Engineers. 2003;**4**:115-125

[24] Gartner J, Cannon S, Santi P. Empirical models for predicting volumes of sediment deposited by debris flows and sediment laden floods in the transverse ranges of southern California. Engineering Geology. 2014;**176**:45-56

[25] Douvinet J, Van de Wiel M, Delahaye D, Cossart E. A flash flood hazard assessment in dry valleys (northern France) by cellular automata modeling. Natural Hazards. 2014;**75**(3):2905-2929. DOI: 10.1007/s11069-014-1470

[26] Delahaye D, Guermond Y, Langlois P. Spatial interaction in the runoff process. In: Proceedings of the 12th ECTG2001, European Colloquium on Theoretical and Quantitative Geography, Saint-Valéry-en-Caux, France. 2001

[27] Langlois P, Delahaye D. Ruicells, un automate cellulaire pour la simulation du ruissellement de surface. Revue Internationale de Géomatique. 2002;**12**:461-487

[28] Kean J, McGuire L, Rengers F, Smith J, Staley D. Amplification of post wildfire peak flow by debris. Geophysical Research Letters. 2016;**43**:8545-8553. DOI: 10.1002/2016GL069661

[29] Keller E, Adamaitis C, Alessio P, Anderson S, Goto E, Gray S, et al. Applications in geomorphology. Geomorphology. 2019;**366**:19. DOI: 10.1016/j.geomorph.2019.04.001

[30] Stock J, Dietrich W. Valley incision by debris flows: Evidence of a topographic signature. Water Resources Research. 2003;**39**(4):1089-1109. DOI: 10.1029/2001WR001057

[31] Kean J, Stanley D, Cannon S. In situ measurements of post-fire debris flows in southern California: Comparisons of the timing and magnitude of 24

debris-flow events with rainfall and soil moisture conditions. Journal of Geophysical Research. 2011;**116**:F04019. DOI: 10.1029/2011JF002005

[32] Santi P, deWolfe V, Higgins J, Cannon S, Gartner J. Sources of debris flow material in burned areas. Geomorphlogy. 2008;**96**:310-321

[33] BAER (U.S. Forest Service Burned Area Emergency Response). Thomas Fire Burn Area Reports, Online. 2018

[34] U.S. Geological Survey. Emergency assessment of post-fire debris-flow hazards, 2017 Thomas Fire, Online. 2018

[35] Restrepo P, Jorgensen D, Cannon S, Costa J, Laber J, Major J, et al. Joint NOAA/NWS/USGS prototype debris flow warning system for recently burned areas in southern California. Bulletin of the American Meteorological Society. 2008;**89**:1845-1851. DOI: 10.1175/2008BAMS2416.1

[36] NWS (National Weather Service). Flash flood and debris flow event, Montecito, California, January 9, 2018; Los Angeles, Oxnard, California, Online.

[37] Bessette-Kirton E, Kean J, Coe J, Rengers F, Staley D. An evaluation of debris-flow runout model accuracy and complexity in Montecito, California: Towards a framework for regional inundation-hazard forecasting. In: Kean JW, Coe JA, Santi PM, Guillen BK, editors. Debris-Flow Hazards Mitigation: Mechanics, Monitoring, Modeling, and Assessment, Proceedings of the 7th International Conference on Debris Flow Hazards Mitigation, Association of Environmental & Engineering Geologists Special Publication. Vol. 28. 2019. pp. 257-264

[38] Hamilton M, Serna J. Montecito Braced for Fire, But Mud Was a More Stealthy. Los Angeles Times: Deadly Threat; 2018

[39] Lai V, Tsai V, Lamb M, Ulzio T, Beer A. The seismic signature of debris flows: Flow mechanics and early warning at Montecito, California. Geophysical Research Letters. 2018, 2018;**45**:5528-5535. DOI: 10.1029/2018GL077683

[40] Langdon S, Johnson A, Sharma R. Debris flow syndrome: Injuries and outcomes after the Montecito Debris flow. The American Surgeon. 2019;**85**:1094-1098. DOI: 10.1177/000313481908501004

[41] Robert D, Niehaus I. The economic impacts of the Montecito Mudslides: First Assessment. 2018. Online

[42] Magnoli G. County estimates $46 million cost for Thomas fire, repairs. 2018

[43] Rodriguez-Iturbe I, Rinaldo A. Fractal River Basins, Chance and Self-organization. Cambridge: Cambridge University Press; 1997. p. 547. DOI: 10.1063/1.882305

[44] Fonstad M. Cellular automata as analysis and synthesis engines at the geomorphology-ecology interface. Geomorphology. 2006;**77**:217-234. DOI: 10.1016/j.geomorph.2006.01.006

[45] Palacios-Vélez O, Gandoy-Bernasconi W, Cuevas-Renaud B. Geometric analysis of surface runoff and the computation order of unit elements in distributed hydrological models. Journal of Hydrology. 1998;**211**:266-274

[46] Shreve R. Statistical law of stream numbers. Journal of Geology. 1966;**74**:17-37. DOI: 10.1086/627137

[47] Bak P. How Nature Works: The Science of Self-organized Criticality. New York: Springer-Verlag; 1996

[48] Murray A, Paola C. A cellular model of braided rivers. Nature. 1994;**371**:54-57

[49] Douvinet J, Serra-Llobet A, Radke J, Kondolf M. Quels enseignements tirer des coulées de débris post-incendie survenues le 9 janvier 2018 à Montecito (Californie, USA)? La Houille Blanche. 2020;**6**:25-35. DOI: 10.1051/lhb/2020052

[50] CAL Fire. Damage inspection database: California Department of Forestry and Fire Protection, Office of the State Fire Marshall, GIS file dated 26 April 2018. 2018

[51] Santa Barbara County. Santa Barbara County Department of Public Works rainfall data Online. 2018